A Multiscale Anomaly Detection Framework for AIS Trajectories via Heat Graph Laplacian Diffusion

Kareth León-López
IRIT/ENSEEIHT/TéSA
University of Toulouse
Toulouse, France

Serge Fabre
TéSA Laboratory
Toulouse, France

Fabio Manzoni, Laurent Mirambell
Hensoldt Nexeya France
Toulouse, France

Jean-Yves Tourneret
IRIT/ENSEEIHT/TéSA
University of Toulouse
Toulouse, France

***Abstract*—The monitoring of abnormal ship behavior is an important task for maritime surveillance for which the automatic identification system (AIS) has been widely exploited. Several works have proposed graph-based anomaly detection (AD) methods on spatial AIS points to provide further information regarding the interactions between the observed data through graph structures. This paper studies a new AD framework on graphs constructed from AIS trajectories. This framework considers a diffusion kernel at multiple scales of the graph Laplacian matrix, referred to as multiscale AD for AIS trajectories (MAD-AIS). MAD-AIS builds an attributed graph from a set of AIS trajectories, where nodes encode spatio-temporal trajectories and edges connect them via a similarity measure. In a second stage, AD is performed by computing scaled versions of the graph Laplacian matrix that are used to assess the graph connectivity. Simulation results are first conducted on synthetic data with controlled ground truth showing that the proposed MAD-AIS can effectively detect the abnormal behavior of ships in terms of spatio-temporal irregularities. Simulations conducted on real AIS subtrajectories (i.e., segments of AIS trajectories) show that abnormal features/attributes can be localized along AIS paths.**

***Index Terms*—Graph anomaly detection, multiscale diffusion graph, automatic identification system, maritime surveillance**

I. Introduction

Data from the automatic identification system (AIS) is collected from vessels and record the dynamic and static information of the ships. Anomaly detection (AD) based on AIS trajectories is nowadays a relevant research field for maritime surveillance [1]–[4]. Different state-of-the-art approaches focus on modeling and extracting the sailing routes or normal traffic patterns from historical AIS data [5]. By modeling vessel behavior as graphs, where nodes correspond to positions and edges capture spatial and temporal connections, graph-based methods have resulted in powerful frameworks for detecting anomalies in maritime traffic [1], [3], [6].

Heat diffusion on graphs has been studied for optimal data embedding in manifolds and for measuring the graph connectivity via the heat equation [7], [8]. In the context of AD, the diffusion process via the heat kernel can be leveraged to identify anomalous nodes in the graph. Nodes that exhibit unusual rapid or high energy concentration compared to their neighbors may indicate anomalous behavior or structural irregularities within the graph [9]–[11]. However, up to our knowledge, there are no previous studies considering this diffusion concept for AD in spatio-temporal trajectories using graphs to analyze their behavior.

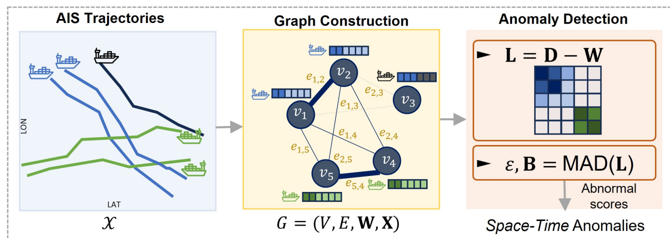

Fig. 1. Multiscale anomaly detection for AIS trajectories (MAD-AIS) framework, where spatio-temporal trajectories (*left*) are encoded on graph nodes V and connected by edges E given by a similarity node measure, yielding the graph G (*center*). The data-based graph is then input to the MAD algorithm for detecting space-time deviated trajectories exploiting the Laplacian matrix of the graph (*right*). Abnormal scores indicate the potential abnormal trajectories.

This paper investigates a new graph-based AD framework to analyze spatio-temporal AIS trajectories. These trajectories are encoded in a graph structure for the detection of potential abnormal paths by heat diffusion on an appropriate graph Laplacian matrix. The Laplacian matrix captures the correlation between trajectories via node adjacency and the attributes or characteristics input to the graph. Then, using scaled versions of the Laplacian through the localized heat kernel at a specific node enables the quantification of dense or weakly connected nodes relative to the entire network graph. The proposed methodology is evaluated using both synthetic and real trajectories. In the real-world scenario, an additional step is implemented to address the issue of having different trajectory lengths. Spatio-temporal subtrajectories are extracted as a set of of trajectory segments that can be processed using the proposed framework.

Figure 1 summarizes the proposed MAD-AIS framework divided into a graph trajectory construction and a multiscale anomaly detection (MAD). Note that the constructed graph is geo-spatio-temporal dependent, representing and modeling actual trajectories from the dataset, while state-of-the-art graphs models the most common stay point of vessels. The contribu-

ISBN: 978-9-4645-9361-7

tions of this paper are twofold: first, a graph representation for modeling spatio-temporal trajectories within a graph structure is proposed to capture the route vessel behavior. In a second step, the effectiveness of the heat diffusion concept for AD in AIS data is evaluated, which is of interest for maritime surveillance.

II. Related Work

A. Anomaly Detection for Ship Trajectories

Several works have presented solutions based on machine learning or statistical methods to detect anomalous behavior in ship trajectories using, for example, AIS or radar data. Anomaly detectors can be either point-based, following clustering methods such as K-means or DBSCAN (density-based spatial clustering of applications with noise) [12] or trajectory-based, where the clustering is performed on the entire trajectories based on similarity measures [13]. Furthermore, classical AD methods have been adapted to detect anomalies in trajectories such as one-class support vector machines [14], isolation forest [3], among others.

B. Graph Anomaly Detection (GAD)

Graphs have been used to represent the structural/relational information, in which nodes/vertices represent objects and edges characterize their relationships. Graph anomaly detection (GAD) aims at exploiting this structural information to detect abnormal graph objects (nodes, edges, subgraphs) [15]. AD on graph-structured data can be done via deep learning techniques, where large and labeled datasets are required [15]. Alternatively, statistical models, matrix factorization and k-nearest neighbors have been used to extract structural patterns for detecting anomalous nodes [15]–[17]. On the other hand, spectral graph analysis has also been exploited for finding anomalies, where the Laplacian matrix is the central subject of the analysis [18]. In this line, a multiscale graph-based AD was studied in [10] to detect anomalies at different neighborhood levels, i.e., locally or globally, with respect to multiples scales.

C. From trajectories to graph structure

Ship trajectories are not naturally graph structured. Thus, one should analyze what is the most representative characteristic from the underlying data that provides a significant feature vector for detecting anomalies in trajectories and then build the graph considering this feature vector. A graph can be built from the data in different ways in order to promote the detection of anomalies. Abnormal ship trajectories are usually associated with the positions of ships, hence, state-of-the-art methods rely on a graph built from the spatial data, i.e., longitude and latitude information. However, there are also anomalies related to the speed, travel time, among others [1], [4], [6]. Typical spatial-related anomalies include the deviation from a standard route, two vessels having too close trajectories, at a given time, or vessels entering restricted areas such as marine protected areas or exclusions zones [2].

In the literature, there are mainly two strategies for constructing an undirected graph from trajectories. A *point-based similarity/distance* strategy that relies on the distance or similarity measure between the data points, and a strategy based on *spatial grids*, which considers that the trajectory lies on a spatial grid to map each trajectory point to a point within the grid [19]. Other strategies considered in the literature seek to learn or estimate the graph structure from the data using an optimization problem [3].

D. GAD for AIS Trajectories

Different approaches have shown the interest of exploiting graphs for detecting abnormal AIS trajectories [1], [3], [20]. In [3], a trajectory graph-based representation is employed to construct maritime routes that vessels are likely to traverse. An abnormal behavior regarding these routes is detected by using a Rayda criterion on the spatial positions and the isolation forest algorithm on the route attributes (such as speed or acceleration). Graphs can also be used to represent the connection between vessels [1]. The graph edges jointly with the AIS data can then be fed into a recurrent neural network to detect different kinds of anomalies including unusual vessel turns, loss of the AIS signal, and AIS anomalous trajectories.

III. Multiscale AD for AIS Trajectories

A. Embedding Trajectories in Graphs

AIS data store vessel information such as ship identifier (ID), longitude (lon), latitude (lat), speed over ground (sog), course over ground (cog), a coordinate universal timestamp (time), and others. Formally, an AIS trajectory can be expressed as a sequence $\{\boldsymbol{x}_1, ..., \boldsymbol{x}_T\}$ of T consecutive discrete state vectors describing the vessel state, where at a given time instant $t \in \{1, ..., T\}$, the vector can be defined as $\boldsymbol{x}_t = [\text{lon}, \text{lat}, \text{cog}, \text{sog}, \text{time}]^\top$, with $\boldsymbol{x}_t \in \mathbb{R}^d$, where d is the number of features. For N trajectories, let $\mathcal{X} \in \mathbb{R}^{N \times T \times d}$ denotes the set of time-features containing the AIS data.

Graph Definition. Considering N trajectories, let $G = (V, E, \mathbf{W})$ denote an undirected weighted graph constructed from the set of trajectories, in which an AIS trajectory is mapped to a node $v_i \in V$, where $V = \{v_1, ..., v_N\}$ is a set of N nodes, E is the set of edges, and $\mathbf{W} \in \mathbb{R}^{N \times N}$ is a matrix containing the edge weights (with $[\mathbf{W}]_{i,i} = 0, \forall i = 1, ..., N$). The degree of the graph $\mathbf{D} \in \mathbb{R}^{N \times N}$ is a diagonal matrix whose ith element is the sum of all edge weights incident to a node i, i.e., $\mathbf{D}_{i,i} = \sum_{j=1}^{N} [\mathbf{W}]_{i,j}$.

Attributed Graph. An attributed/weighted graph is defined as $G = (V, E, \mathbf{W}, \mathbf{X})$, with node attributes $\mathbf{X} = \{\mathbf{x}_1, ..., \mathbf{x}_N\}$, with $\mathbf{x}_n \in \mathbb{R}^M$, and M is the dimension of the attributes. The weighted adjacency matrix is then defined using a similarity measure between the attributes as

$$[\mathbf{W}]_{u,v} = \begin{cases} \exp\left(-\frac{\|\mathbf{X}_u - \mathbf{X}_v\|^2}{2\sigma^2} \right), & \text{if } (u,v) \in E \\ 0, & \text{otherwise,} \end{cases} \quad (1)$$

where σ is the standard deviation of the attributes in the set $\mathbf{X}$. In practice, the edge set E is built via the well-known ϵ-graph, where two nodes are connected if a given distance or similarity measure is less than a threshold ϵ. Finally, the graph

Laplacian matrix is defined in terms of the degree and weight matrices as $\mathbf{L} = \mathbf{D} - \mathbf{W}$, where $\mathbf{L}$ encodes information about the connectivity and structure of the graph [21].

B. Heat Diffusion Kernel for Multiscale Concentration

This paper assumes that weighted edges connect trajectories that are locally/spatially close, where each weight represents a similarity measure between two trajectories of the set. An edge weight $[\mathbf{W}]_{u,v}$ is associated with a *heat energy* that can be measured by localizing a kernel $\mathcal{H}$ at a given node [11]. If the edge weight is large, then, the heat can flow easily between two connected nodes. This concept has been studied in diffusion processes in which the heat equation describes how the energy is diffused over a geometry [11], [22].

It is well-known that the heat equation is solved via the *heat kernel*, which has been expressed in terms of the Laplacian matrix as [21], [22]:

$$\mathcal{H}_\tau = e^{-\tau \mathbf{L}}, \tag{2}$$

where τ represents the scale/time in which the energy is diffused. The heat kernel can be localized at the node $i \in V$ by a delta function δ_i, such that it is possible to measure the connectivity of the node regarding its neighbors as a concentration measure.

The heat concentration at the node i is then defined as the ℓ_2 norm of the heat Kernel $\mathcal{H}$ applied to node i as [11]:

$$\mathbf{\Gamma}_{i,\tau} = \left\| e^{-\tau \mathbf{L}} \delta_i \right\|_2, \tag{3}$$

where τ belongs to a set of scales $\{\tau_1, ..., \tau_R\}$. Then, relatively high concentrations measured in (3) will indicate weakly connected nodes, i.e., trajectories that are potentially dissimilar to most trajectories. To detect the nodes with high concentration in the graph, a detector is defined as:

$$\mathbf{B}_{i,\tau} = \begin{cases} 1, & \text{if } \mathbf{\Gamma}_{i,\tau} \geq \kappa_\tau \\ 0, & \text{otherwise} \end{cases}, \text{ for } \tau \in \{\tau_1, ..., \tau_R\}, \tag{4}$$

where $\kappa_\tau = \mu_{\mathbf{\Gamma}_\tau} + 2\sigma_{\mathbf{\Gamma}_\tau}$ is a threshold given in terms of the mean $\mu_{\mathbf{\Gamma}_\tau}$ and standard deviation $\sigma_{\mathbf{\Gamma}_\tau}$ of the values of $\mathbf{\Gamma}_{i,\tau}$ [10]. Then, different scale values at a given node i lead to measure its connectivity locally and globally in the graph [10], [11]. Finally, a multiscale abnormal score can be computed to rate the abnormality level of each node as $\varepsilon_i = \frac{1}{R}\sum_{\tau=\tau_1}^{\tau_R} \mathbf{B}_{i,\tau}$, such that $\boldsymbol{\varepsilon} \in [0,1]^N$. Algorithm 1 summarizes the steps for computing the multiscale abnormal score using a diffusion on the Laplacian matrix.

Algorithm 1: MAD: Multiscale AD via Heat Diffusion

Input : Laplacian matrix $\mathbf{L} \in \mathbb{R}^{N \times N}$, scale values $\{\tau_1, ..., \tau_R\}$, number of nodes N
Output: Abnormal node scores $\boldsymbol{\varepsilon} \in \mathbb{R}^N$, $\mathbf{\Gamma} \in \mathbb{R}^{N \times R}$

for $i = 1$ **to** N **do**
  for $\tau = \tau_1$ **to** τ_R **do**
    $\mathbf{\Gamma}_{i,\tau} = \left\| e^{-\tau \mathbf{L}} \delta_i \right\|_2$
  $\kappa_\tau = \mu_{\mathbf{\Gamma}_\tau} + 2\sigma_{\mathbf{\Gamma}_\tau}$
  Compute $\mathbf{B}$ using Eq. (4)
  $\varepsilon_i = \frac{1}{R}\sum_{\tau=\tau_1}^{\tau_R} \mathbf{B}_{i,\tau}$

IV. Simulation Results

To evaluate the proposed framework for graph construction and graph AD, experimental results on both synthetic and real-world data sets are conducted.

A. Experimental Setup

Datasets. The synthetic dataset of [14] is first considered. This dataset contains randomly generated trajectories gathered in $N = 1000$ sets. Each set contains 260 trajectories: 250 normal trajectories grouped in 5 main rails or routes, and 10 outliers. An individual trajectory has 16 points defined as pairs of spatial coordinates (x, y). The performance of the proposed framework is evaluated on the first 600 trajectories from the whole set.

A publicly available real dataset is also considered [23]. This dataset contains AIS winter vessel trajectories recorded in years 2017-2019 from the Baltic Sea. These trajectories were used to evaluate the proposed framework for graph construction and AD. The dataset was preprocessed by the following two steps: 1) AIS trajectories belonging to the same vessel (i.e., data with the same ship ID number) but exhibiting atypical behaviors were separated, 2) a trajectory was divided into two parts if, at a specific time, a vessel has a distance to the coast equal to less than 20 km while the time difference between two consecutive AIS messages is greater that 2 hours. These rules ensure that trajectories from the same vessel makes sense. After this preprocessing step, a set of 80 trajectories with different numbers of spatio-temporal AIS observations/points was obtained. Figure 4 (a) displays the set of AIS trajectories on a map.

Metrics. There is a groundtruth for the synthetic dataset. Thus, the AD performance is quantified using the well-known precision, recall and $F1$-score metrics, which are defined in terms of true positive (TP), true negative (TN), false positive (FP), and false negative (FN) values. On the other hand, the results were qualitatively analyzed for the real dataset.

State-of-the-art methods. The proposed framework is compared against some standard AD methods such as DBSCAN and local outlier factor (LOF), which are adapted for trajectory-based AD via a trajectory distance matrix [24]. The DBSCAN method is a clustering method designed to identify dense regions measured by the number of objects close to a given point. The two hyperparameters that need to be adjusted in DBSCAN are *eps*, defining the radius of the neighborhood around a point, and *MinPts*, representing the minimum number of neighbors within the *eps* radius. On the other hand, the LOF method measures the local density deviation of each observation with respect to its k nearest neighbors. LOF uses two hyperparameters: the neighborhood size k_{LOF} and the contamination γ, which specifies the amount of contamination or proportion of outliers in the dataset. Regarding the input parameters to MAD algorithm, the scale range is set to a sequence of 200 evenly spaced numbers over the interval $[0, 1000]$ and the number of nodes N is set accordingly to the dataset under analysis.

B. Synthetic Results

In the synthetic scenario, the constructed graph has 260 nodes and the number of edges depends on the specific dataset. The graph weights are computed as in Eq. (1) with node attributes defined as the (x, y, t) spatio-temporal points of the trajectory. Spatio-temporal deviating trajectories with respect to all the trajectories from the dataset are detected as abnormal nodes in the graph. Table I illustrates a mean and standard deviation (STD) performance comparison of the AD methods, in which MAD-AIS exhibits slightly higher recall rates, resulting in superior average F1-scores. Note that the concurrent AD methods are highly competitive state-of-the-art detectors.

TABLE I
PERFORMANCE COMPARISON OF DIFFERENT AD METHODS.

	Precision		Recall		F1-score	
Method	MEAN	STD	MEAN	STD	MEAN	STD
MAD-AIS	**0.9875**	**0.0220**	**0.9687**	0.0388	**0.9767**	**0.0255**
DBSCAN	0.9795	0.0284	0.9678	0.0413	0.9722	0.0283
LOF	0.9817	0.0266	0.9645	**0.0379**	0.9724	0.0309

Detection performance for specific trajectory subsets. The two subsets #100 and #540, displayed in Fig. 2, have been selected from the synthetic set of trajectories to illustrate the detection performance. The performance for these subsets is shown in Tables II and III, where the FN and FP rate are provided for the different methods. The parameters used in each method are shown in parenthesis, precisely, DBSCAN (*eps*; *MinPts*), and LOF (k_{LOF},γ).

Figure 3 illustrates the multiscale trajectory concentrations for the subset #540 at (a-b) two given scales and (c) the multiscale ε scores, where the colors show the level of abnormality that is given between 0 and 1: the closer to 1 (red), the more abnormal.

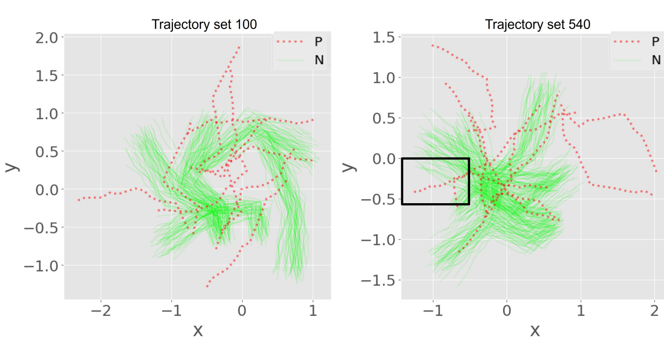

Fig. 2. Trajectory subsets #100 and #540 from the synthetic dataset [14]. The red dotted curves show the abnormal trajectories (positives) while the green lines are the normal ones (negatives).

C. Application to Real Data

To apply the MAD-AIS framework on real data (shown in Fig. 4-(a)), due to the diversity of trajectories depending

TABLE II
PERFORMANCE COMPARISON FOR THE SUBSET #100.

Method (params)	FN	FP	Precision	Recall	F1-score
MAD-AIS	1	0	**0.998**	**0.95**	**0.9727**
DBSCAN (0.2;2)	1	1	0.948	0.948	0.948
LOF (9;1/26)	1	1	0.948	0.948	0.948

TABLE III
PERFORMANCE COMPARISON FOR THE SUBSET #540.

Method (params)	FN	FP	Precision	Recall	F1-score
MAD-AIS	2	0	**0.996**	**0.9**	**0.943**
DBSCAN (0.2;2)	3	0	0.994	0.85	0.909
LOF (9;1/26)	1	2	0.940	0.898	0.918

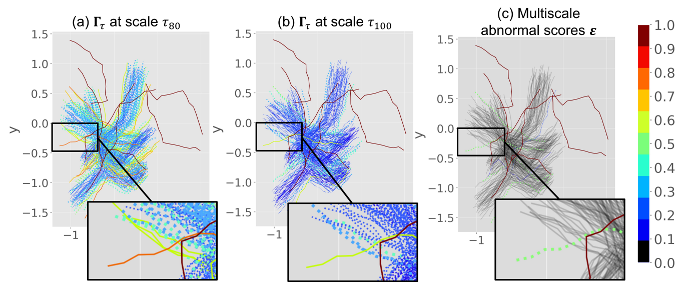

Fig. 3. Trajectory concentration for the subset #540 using (3) at the scale (a) τ_{80} and (b) τ_{100}, and (c) the multiscale abnormal score, where the scores (0,1) are mapped to the colors given the color bar (the closer to 1, the more abnormal). The zoomed section shows a slightly deviated trajectory, which is ranked as abnormal at different scales and its true label is shown in a black rectangle in Fig. 2.

on the type of ship and route, we propose to analyze the trajectories by segments, leading to different attribute sizes for each node. This segment-based analysis also allows anomalies to be localized along the path to detect in which part of the trajectory the anomaly is present. Segments can be extracted from the real trajectories by two manners: segments from a sliding window (SW) or from the Ramer–Douglas–Peucker algorithm (RDP) [25]. The multiscale abnormal scores ε for the real trajectories using the two segmentations are displayed in Fig. 4 (b-c), where the SW is fixed to a non-overlapping window size of 32 points and the colors in the plot show the level of abnormality. The abnormality scores highlight the deviating segments or subtrajectories of the set that are likely to be abnormal regarding the main rail trajectories (i.e., the central trajectories marked in black).

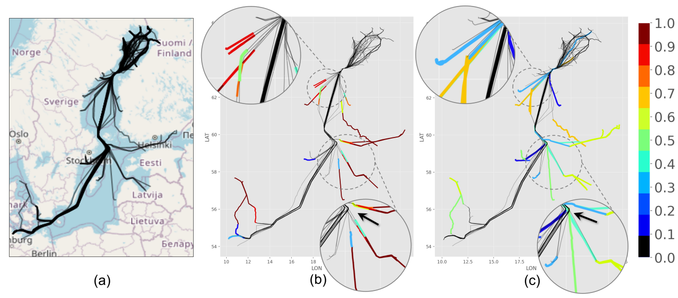

Fig. 4. (a) Baltic sea AIS trajectories and the MAD-AIS scores ε when (b) the nodes are encoded by considering subtrajectories from SW segments and (c) from the RDP segmentation, where the colors in the plot show the level of abnormality. Zoomed sections show deviated trajectory segments, where the arrows indicate that RDP-based segments promote the detection of the segment path after it starts to deviate.

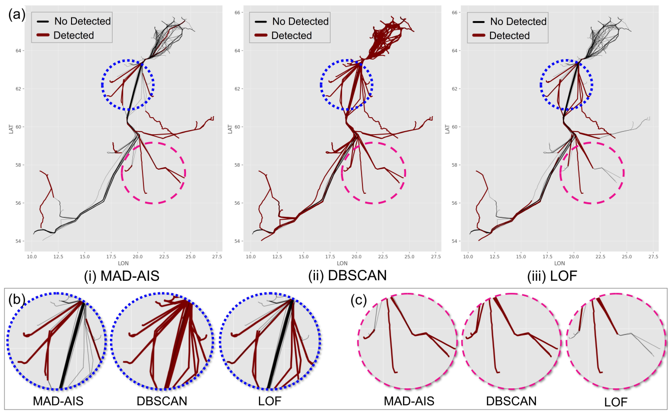

Fig. 5. (a) AD result comparison of the MAD-AIS detection against DBSCAN and LOF. (b-c) Highlighted parts show some detected deviated paths in red, where DBSCAN misidentifies main rails as abnormal (b-DBSCAN) and LOF overlooks significant deviated portions.

Figure 5 shows the AD result comparison using the three methods on RDP-based segments, where the encircled zoom parts highlight spatio-temporal deviations from the main trajectory rails (marked in red) and, the MAD-AIS shows the detection by setting the abnormality scores to a fixed threshold equal to 0.1, for comparison purposes. From the highlighted parts in Fig. 5(b-c), one can observe that DBSCAN and LOF are inconsistent since, for example, the main rail is marked as an anomaly when using DBSCAN, Fig. 5(b-DBSCAN), and highly deviated parts are not detected using LOF zoom, Fig. 5(c-LOF).

V. Conclusions

This paper studied a graph-based anomaly detection framework for ship trajectories using AIS data, referred to as MAD-AIS. MAD-AIS provides an effective way to evaluate the connectivity of a vessel-based graph in which trajectories are encoded. The performance of the proposed AD method was assessed on synthetic and real datasets. Particularly noteworthy is its adaptability demonstrated with real-world data, where the approach not only detects anomalous trajectories but also identifies subtrajectories deviating from the dominant paths via subtrajectory analyses. Future work includes exploring other AIS features (such as speed, direction, angle) encoded on attributed AIS graphs for detecting other kinds of abnormal trajectories. Generalizing the proposed framework to handle labelled/unlabelled data would also be interesting.

References

[1] S. K. Singh, J. S. Fowdur, J. Gawlikowski, and D. Medina, "Leveraging graph and deep learning uncertainties to detect anomalous maritime trajectories," *IEEE Transactions on Intelligent Transportation Systems*, vol. 23, no. 12, pp. 23 488–23 502, 2022.

[2] K. Wolsing, L. Roepert, J. Bauer, and K. Wehrle, "Anomaly detection in maritime AIS tracks: A review of recent approaches," *Journal of Marine Science and Engineering*, vol. 10, no. 1, p. 112, 2022.

[3] Y. Shi, C. Long, X. Yang, and M. Deng, "Abnormal ship behavior detection based on AIS data," *Applied Sciences*, vol. 12, no. 9, p. 4635, 2022.

[4] T. Stach, Y. Kinkel, M. Constapel, and H.-C. Burmeister, "Maritime anomaly detection for vessel traffic services: A survey," *Journal of Marine Science and Engineering*, vol. 11, no. 6, p. 1174, 2023.

[5] L. Eljabu, M. Etemad, and S. Matwin, "Spatial clustering model of vessel trajectory to extract sailing routes based on AIS data," *International Journal of Computer and Systems Engineering*, vol. 16, no. 10, pp. 491–501, 2022.

[6] Z. Yan, Y. Xiao, L. Cheng, R. He, X. Ruan, X. Zhou, M. Li, and R. Bin, "Exploring AIS data for intelligent maritime routes extraction," *Applied Ocean Research*, vol. 101, p. 102271, 2020.

[7] D. Thanou, X. Dong, D. Kressner, and P. Frossard, "Learning heat diffusion graphs," *IEEE Transactions on Signal and Information Processing over Networks*, vol. 3, no. 3, pp. 484–499, 2017.

[8] F. Zhang and E. R. Hancock, "Graph spectral image smoothing using the heat kernel," *Pattern Recognition*, vol. 41, no. 11, pp. 3328–3342, 2008.

[9] J. Huang and Y. Yang, "Anomaly detection in machining centers based on graph diffusion-hierarchical neighbor aggregation networks," *Applied Sciences*, vol. 13, no. 23, p. 12914, 2023.

[10] L. Gutiérrez-Gómez, A. Bovet, and J.-C. Delvenne, "Multi-scale anomaly detection on attributed networks," in *Proc. AAAI conference on artificial intelligence*, vol. 34, no. 1, New-York, NY, 2020, pp. 678–685.

[11] N. Perraudin, B. Ricaud, D. I. Shuman, and P. Vandergheynst, "Global and local uncertainty principles for signals on graphs," *APSIPA Transactions on Signal and Information Processing*, vol. 7, p. e3, 2018.

[12] B. Zhang, K. Hirayama, H. Ren, D. Wang, and H. Li, "Ship anomalous behavior detection using clustering and deep recurrent neural network," *Journal of Marine Science and Engineering*, vol. 11, no. 4, p. 763, 2023.

[13] G. Pallotta and A.-L. Jousselme, "Data-driven detection and context-based classification of maritime anomalies," in *Proc. International Conference on Information Fusion (Fusion)*, Washington, DC, 2015, pp. 1152–1159.

[14] C. Piciarelli, C. Micheloni, and G. L. Foresti, "Trajectory-based anomalous event detection," *IEEE Transactions on Circuits and Systems for video Technology*, vol. 18, no. 11, pp. 1544–1554, 2008.

[15] X. Ma, J. Wu, S. Xue, J. Yang, C. Zhou, Q. Z. Sheng, H. Xiong, and L. Akoglu, "A comprehensive survey on graph anomaly detection with deep learning," *IEEE Transactions on Knowledge and Data Engineering*, vol. 35, no. 12, pp. 12 012–12 038, 2023.

[16] N. Liu, X. Huang, and X. Hu, "Accelerated local anomaly detection via resolving attributed networks." in *IJCAI*, 2017, pp. 2337–2343.

[17] Z. Peng, M. Luo, J. Li, H. Liu, Q. Zheng *et al.*, "ANOMALOUS: A joint modeling approach for anomaly detection on attributed networks." in *IJCAI*, 2018, pp. 3513–3519.

[18] S. Calderara, U. Heinemann, A. Prati, R. Cucchiara, and N. Tishby, "Detecting anomalies in people's trajectories using spectral graph analysis," *Computer Vision and Image Understanding*, vol. 115, no. 8, pp. 1099–1111, 2011.

[19] S. Luo, W. Zeng, and B. Sun, "Contrastive learning for graph-based vessel trajectory similarity computation," *Journal of Marine Science and Engineering*, vol. 11, no. 9, p. 1840, 2023.

[20] P.-R. Lei, "A framework for anomaly detection in maritime trajectory behavior," *Knowledge and Information Systems*, vol. 47, no. 1, pp. 189–214, 2016.

[21] A. Ortega, P. Frossard, J. Kovačević, J. M. Moura, and P. Vandergheynst, "Graph signal processing: Overview, challenges, and applications," *Proceedings of the IEEE*, vol. 106, no. 5, pp. 808–828, 2018.

[22] D. I. Shuman, S. K. Narang, P. Frossard, A. Ortega, and P. Vandergheynst, "The emerging field of signal processing on graphs: Extending high-dimensional data analysis to networks and other irregular domains," *IEEE signal processing magazine*, vol. 30, no. 3, pp. 83–98, 2013.

[23] V. Hakola, "Vessel tracking (AIS), vessel metadata and dirway datasets," 2020. [Online]. Available: https://dx.doi.org/10.21227/j3b5-es69

[24] Z. Wang, J. Hu, and Q. Fan, "Extracting the main routes and speed profiles between two locations from massive uncertain historical trajectories," in *2018 International Symposium in Sensing and Instrumentation in IoT Era (ISSI)*. IEEE, 2018, pp. 1–5.

[25] D. H. Douglas and T. K. Peucker, "Algorithms for the reduction of the number of points required to represent a digitized line or its caricature," *Cartographica: the international journal for geographic information and geovisualization*, vol. 10, no. 2, pp. 112–122, 1973.